Key Points:
- Develop an early warning indicator of MOC collapse based on complex networks
- Demonstrate its performance using the data from a GCM that shows MOC collapse
- Formulate optimal observation locations from quality measures of the indicator

Correspondence to:
Q. Y. Feng,
Q.Feng@uu.nl

Deep ocean early warning signals of an Atlantic MOC collapse

Qing Yi Feng[1], Jan P. Viebahn[1], and Henk A. Dijkstra[1]

[1]Institute for Marine and Atmospheric Research Utrecht, Department of Physics and Astronomy, Utrecht University, Utrecht, Netherlands

Abstract A future collapse of the Atlantic Meridional Overturning Circulation (MOC) has been identified as one of the most dangerous tipping points in the climate system. It is therefore crucial to develop early warning indicators for such a potential collapse based on relatively short time series. So far, attempts to use indicators based on critical slowdown have been marginally successful. Based on complex climate network reconstruction, we here present a promising new indicator for the MOC collapse that efficiently monitors spatial changes in deep ocean circulation. Through our analysis of the performance of this indicator, we formulate optimal locations of measurement of the MOC to provide early warning signals of a collapse. Our results imply that an increase in spatial resolution of the Atlantic MOC observations (i.e., at more sections) can improve early detection, because the spatial coherence in the deep ocean arising near the transition is better captured.

1. Introduction

The Atlantic Meridional Overturning Circulation (MOC) is a crucial part of the climate system because of its associated northward heat transport [*Ganachaud and Wunsch*, 2000; *Johns et al.*, 2011]. The present-day MOC is sensitive to freshwater anomalies and may collapse to a state with a strongly reduced northward heat transport [*Bryan*, 1986; *Rahmstorf*, 2000]. It has been identified as one of the important tipping elements in the climate system [*Lenton et al.*, 2008]. Although there are studies which argue that such tipping point events are unlikely to occur within the 21st century [*Tietsche et al.*, 2011], we should be modest in our confidence in this statement as state-of-the-art GCMs have not been extensively tested for this behavior [*Huisman et al.*, 2010; *Collins et al.*, 2013].

Critical slowdown has been a key phrase in the detection of tipping points in ecosystems [*Dakos et al.*, 2011] and the climate system [*Lenton*, 2011]. Indeed, in many natural and man-made systems, there is an increase in response times to perturbations as a tipping point is approached [*Scheffer et al.*, 2009]. The detection of MOC collapses, and the design of early warning signals has so far mostly been based on the analysis of single time series [*Livina and Lenton*, 2007; *Lenton*, 2011]. Critical slowdown induces changes in variance and lag 1 autocorrelation in the time series that can be connected to the distance to the tipping point, and hence, these quantities can serve as early warning indicators [*Scheffer et al.*, 2009].

In this paper, we develop and explore the performance of an early warning indicator of the MOC collapse. One of the novel aspects of this indicator is that it is based on changes in the topology of a complex (interaction) network [*Tsonis and Swanson*, 2006; *Donges et al.*, 2009] constructed from a set of MOC time series. We also determine optimal observation locations through quality measures of the indicator and show that one needs multiple sections in the Atlantic to have a high-quality indicator of the MOC collapse.

2. Data and Methods

Here we use the MOC data from the control simulation and the freshwater-perturbed (from now on referred to as "hosing") simulation of the FAst Met Office/UK Universities Simulator (FAMOUS) climate model. The details of the model are described in *Hawkins et al.* [2011], and for general information we refer to Text S1 of the supporting information (SI). In the hosing simulation, the freshwater flux over the extratropical North Atlantic is increased linearly from zero to 1.0 sverdrup (Sv) (1 Sv = 10^6 m^3 s^{-1}) over 2000 years [*Hawkins et al.*, 2011]. Figure 1a displays the annual mean time series of the Atlantic MOC value at latitude 26°N and at 1000 m depth, the location of the maximum MOC before the collapse, for the control simulation (green curve) and the hosing simulation (blue curve). Whereas the control MOC values are statistically stationary
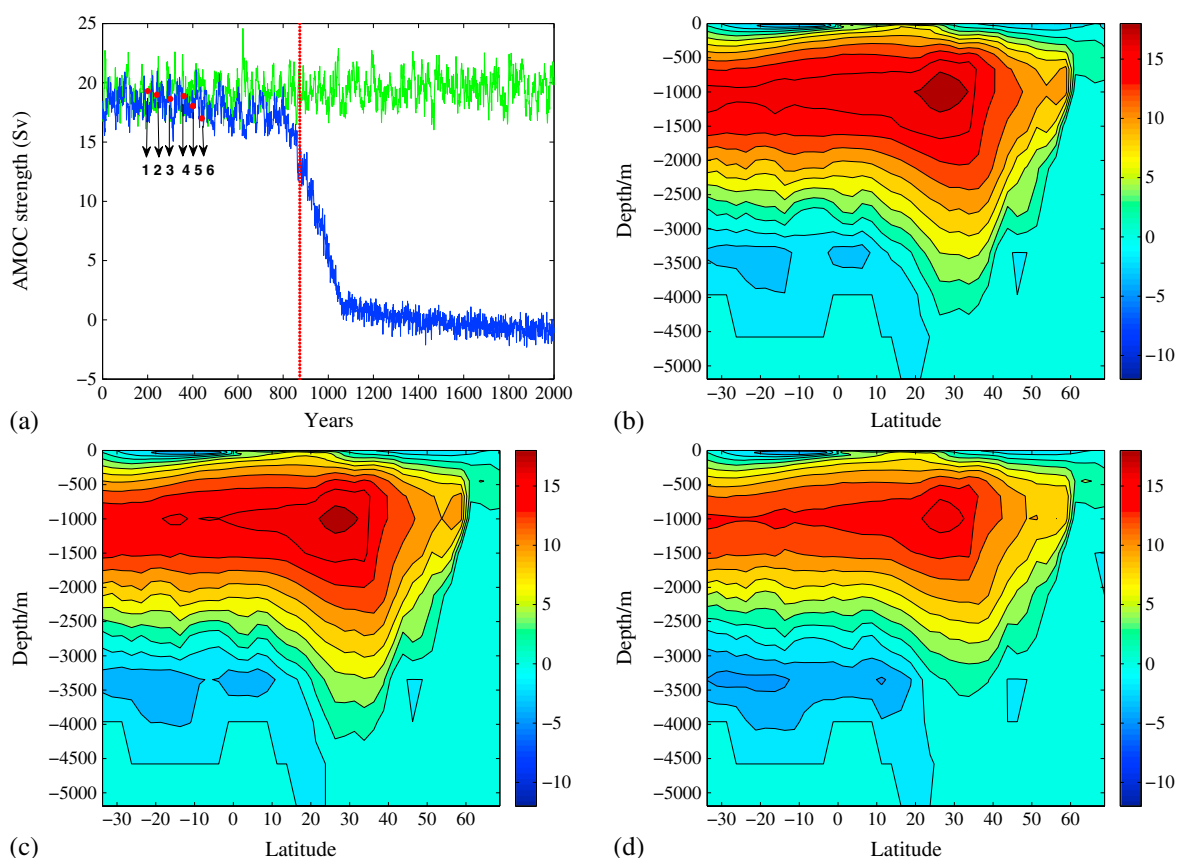
Figure 1. (a) Time series of the MOC (in Sv, 1 Sv = 10^6 m^3 s^{-1}) at 26°N and 1000 m depth in the Atlantic for the control simulation (green curve) and the freshwater-perturbed simulation (blue curve) of the FAMOUS model. The red dots labeled from 1 to 6 show the average values of MOC from the corresponding equilibrium simulations, and the red broken line indicates the collapse time τ_c = 874 years. (b) Annual mean MOC stream function pattern of equilibrium simulation 1. (c) Same as Figure 1b but of equilibrium simulation 4. (d) Same as Figure 1b but of equilibrium simulation 6.

over the 2000 year integration period, the MOC values for the hosing simulation show a rapid decrease between the years 800 and 1050.

We also use the MOC data from the FAMOUS simulations, in which the freshwater flux was fixed after a certain integration time and the model was integrated to equilibrium [*Hawkins et al.*, 2011]. Time series of the MOC of the last 100 years of these simulations were analyzed, and the mean MOC values (again at 26°N and 1000 m depth) are plotted as the red dots labeled from 1 to 6 in Figure 1a. Figures 1b–1d show mean MOC stream function patterns of three of these equilibrium simulations (labelled with 1, 4, and 6 in Figure 1a). Although the equilibrium value of the MOC decreases with larger freshwater inflow, the changes in the MOC pattern are relatively minor. For a slightly higher value of the freshwater flux than the one at point 6, the equilibrium solution is a collapsed state [*Hawkins et al.*, 2011]. In the hosing simulation, the freshwater is, however, added relatively fast compared to the equilibration time scale of the MOC. Hence, the MOC maintains its pattern for much higher freshwater inflow and collapses near 900 years (Figure 1a). To determine a collapse time τ_c more precisely, we use the control simulation of FAMOUS (see Text S2 of the SI). We find τ_c = 874 years, which is shown as the red dashed line in Figure 1a.

Here we build on an idea to use complex network theory to construct an early warning indicator [*Mheen et al.*, 2013]. From the MOC data of the FAMOUS model over the latitudinal domain [35°S–70°N] of the Atlantic Ocean, we construct a Climate Network (CN). The nodes of the network are the latitude depth values of the grid points of the model. A "link" between two nodes is determined by a significant interdependence between their MOC anomaly time series. There are several measures of quantifying the degree of statistical interdependence, and the most common one is calculating the Pearson correlations of pairs of time series [*Tsonis and Roebber*, 2004]. More precisely, in a Pearson Correlation Climate Network (PCCN) [*Feng and Dijkstra*, 2014] an unweighted and undirected link between two nodes exists if the linear Pearson correlation
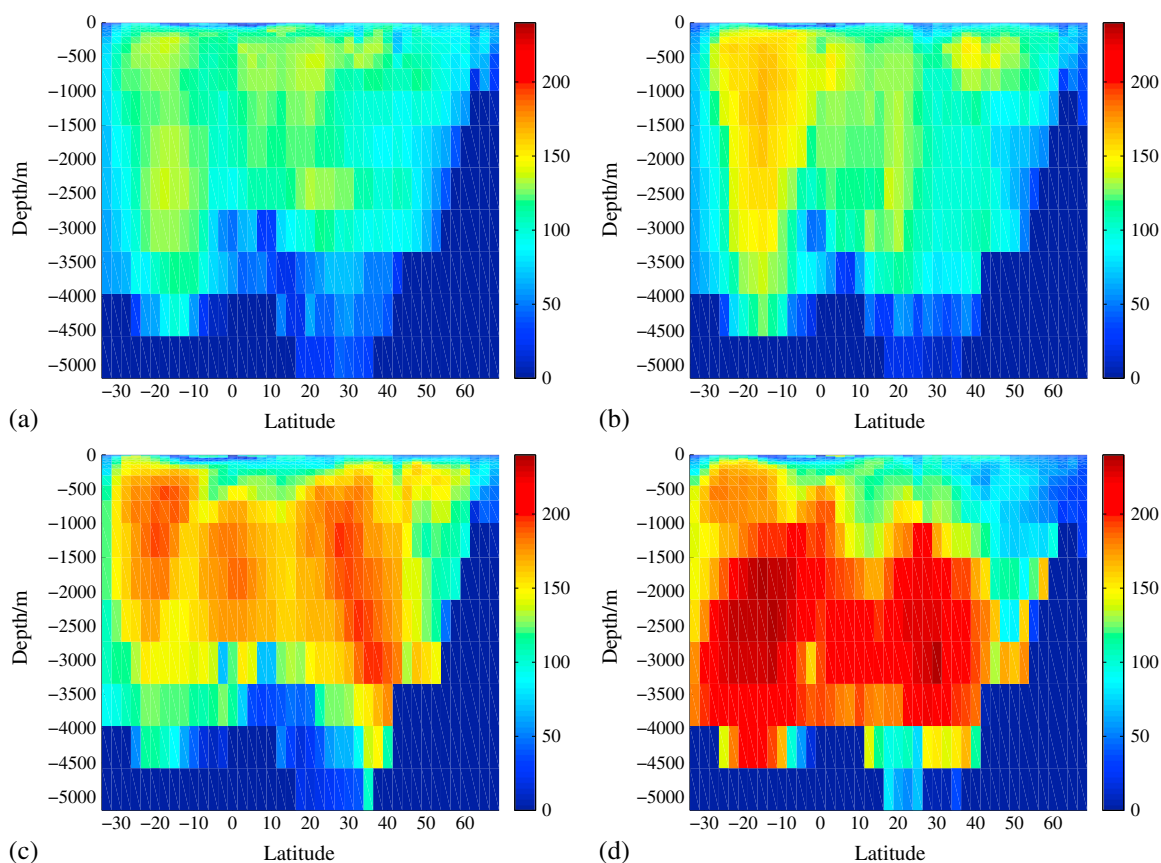
Figure 2. (a) Degree field of the Pearson Correlation Climate Network (PCCN) constructed from the MOC data of equilibrium simulation 1 in Figure 1a using a threshold $\tau = 0.5$. (b) Same as Figure 2a but of equilibrium simulation 2. (c) Same as Figure 2a but of equilibrium simulation 4. (d) Same as Figure 2a of equilibrium simulation 6.

coefficient of the MOC time series at these two nodes exceeds a threshold value such that the correlation is significant ($p = 0.05$).

3. Results

We first construct PCCNs using the complete Atlantic MOC field for each of the six 100 year equilibrium simulations (red dots in Figure 1a). Details on the size of sliding window and threshold values can be found in Text S3 of the SI. For the topological analysis of the PCCNs, we only use the degree field [*Tsonis and Swanson*, 2006; *Donges et al.*, 2009; *Viebahn and Dijkstra*, 2014]. The degree of a node is the number of links between this node and other nodes. As shown in Figure 2 the changes in the degree field at the equilibrium solutions 1, 2, 4, and 6 in Figure 1a are distinct. When the freshwater forcing is increased, high degree in the network—indicating high-spatial MOC correlations—first appears at nodes in the South Atlantic at about 1000 m depth (Figures 2a–2b). It subsequently extends to the whole Atlantic with highest amplitudes in the deep ocean at midlatitudes (Figures 2c–2d).

A similar result was obtained using networks from the temperature field of an idealized spatially two-dimensional model of the MOC [*Mheen et al.*, 2013]. The behavior of the degree field can be understood from the underlying structure of the empirical orthogonal functions (EOFs) of the MOC field (see Text S4 of the SI). Once the transition is approached, one of the EOFs becomes most dominant in the variability. The network can be seen as a coarse graining of the variability, and by focussing only on the largest correlations, it is ideally suited to monitor the changes in the spatial correlations of the system once the transition is approached.

Next, we study the transient behavior of the hosing simulation by constructing similar PCCNs. In *Mheen et al.* [2013], the kurtosis K_d of the degree distribution was introduced as an effective indicator to capture
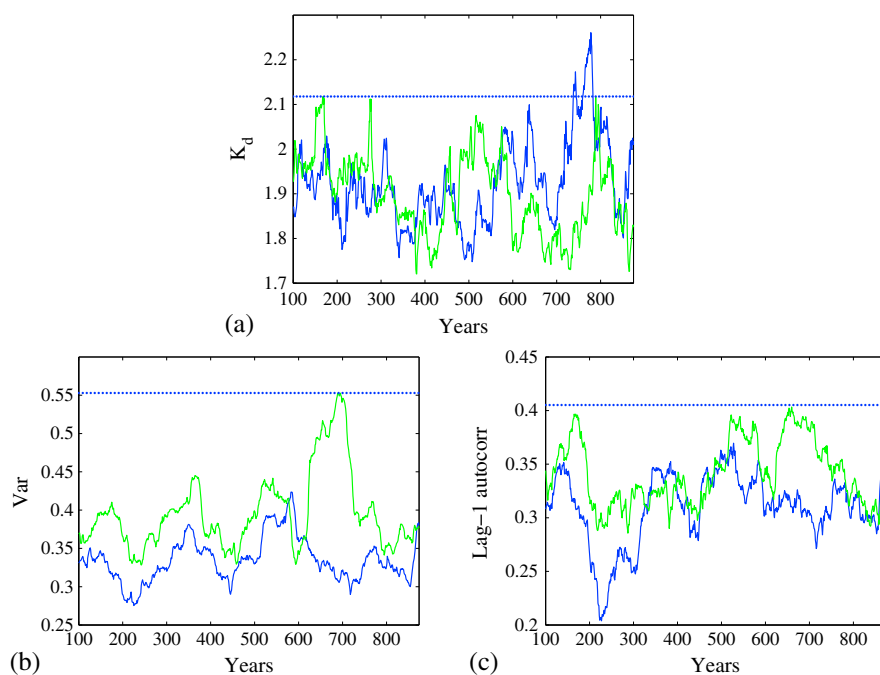
Figure 3. For the complete Atlantic MOC field, (a) the kurtosis indicator K_d gives the early warning signal at 738 years and lasts for 44 years. (b) The traditional variance indicator Var gives no early warning signal before the collapse time $\tau_c = 874$ years. (c) The traditional lag 1 autocorrelation indicator Autocorr gives no early warning signal before the collapse time τ_c. Green solid curves are related to the control simulation, and blue solid curves are related to the hosing simulation. The dashed blue horizontal lines indicate the corresponding maximum values of the control simulation taken over the total time interval $[0, \tau_c]$.

the changes in the topology of the degree field. For the complete Atlantic MOC field, the values of K_d for the hosing simulation (blue curve) and for the control simulation (green curve) are plotted in Figure 3a. For the hosing simulation, there is indeed a strong increase of K_d to values far extending those for the control simulation significantly before the collapse time τ_c. For comparison, the critical slowdown indicator variance (Figure 3b) and lag 1 autocorrelation (Figure 3c) based on the complete Atlantic MOC data (and using the same sliding window) do not show any early warning signal of the MOC transition before the collapse time τ_c.

To provide a measure of the performance of an indicator I, we introduce an evaluation scheme, which consists of the detection time, the reliability of the indication, and the intensity of the indication, γ^I.

1. *Detection time*: When a value of an indicator for the hosing simulation exceeds the maximum of the same indicator for the control simulation, we flag an alarm of a collapse. For example, the maximum of K_d for the control simulation (green curve in Figure 3a) is plotted as the blue dashed line in Figure 3a. In this case, an early warning signal is detected at year 738, which is 136 years before the MOC collapse time $\tau_c = 874$ years.

2. *False alarm*: We label a detection time which is smaller than $\tau_c - 300$ years as a false alarm. The reason we choose this time frame is that in the hosing simulation the system needs about 300 years to adapt to the changes in freshwater flux. This time span is visible in Figure 1a as the time between the system passing the freshwater flux related to equilibrium point 6 and its actual collapse. Moreover, the 300 years is based on the horizon considered in the Fifth Assessment Report of the Intergovernmental Panel on Climate Change (IPCC-AR5) [*Collins et al.*, 2013] for the evolution of the climate system (such as reflected in the Extended Concentration Pathway Emissions and Forcing scenarios, ECPs). Such a time period is also considered to be a political time horizon [*Lenton et al.*, 2008] such that decisions taken within this period are able to affect the occurrence of a collapse. In addition, when the detection time is within $[\tau_c - 300, \tau_c]$, but the signal only lasts less than 5 years, it is also considered as a false alarm.

Table 1. The Performance of the Kurtosis Indicator K_d Based on Complex Networks Constructed From Sets of Section Data at Different Latitudes[a]

No.	Section	Detection Time (Year)	False Alarm	γ^{K_d}
1	(35°S, 70°N, 2.5°)	738	No	0.0675
2	26°N	384/567/868	Yes/Yes/No	0.1031/0.0451/0.0105
3	33°S	-	-	−0.1252
4	(35°S, 70°N, 5°)	739	No	0.0472
5	(20°N, 70°N, 5°)	-	-	0
6	(35°S, 20°N, 5°)	785	No	0.0559
7	(35°S, 35°N, 5°)	785	No	0.0773
8	(20°S, 35°N, 5°)	785	No	0.0584
9	Latitude set I	753	No	0.1248
10	Latitudes set II	740	No	0.0951
11	Latitude set III	-	-	−0.0810
12	Latitude set IV	-	-	−0.0454

[a]In the sets of sections indicated by brackets, the first entry indicates the southern boundary, the second entry the northern boundary, and the third entry is the latitudinal step.
I: 18°S, 13°S, 8°S, 11°N, 16°N, 21°N, 26°N, and 31°N
II: 33°S, 18°S, 13°S, 11°N, 16°N, 21°N, 26°N, and 31°N
III: 13°N, 16°N, 18°N, 21°N, 23°N, 26°N, 28°N, and 31°N
IV: 33°S, 31°S, 28°S, 26°S, 23°S, 21°S, 18°S, and 16°S

3. *Detection intensity* γ^I: The amplitude of the peak of the indicator is also important. Therefore, we additionally define another quality measure γ^I for indicator I as

$$\gamma^I = \frac{\max_P(I^{hosing})}{\max_{[0,\tau_c]}(I^{control})} - 1$$

Here the maximum of the control is taken over the total time interval $[0, \tau_c]$ and that of the hosing only over the peak interval P where the indicator extends over the threshold value. This choice for the control is based on the fact that the FAMOUS model control simulation still displays a slight drift. Hence, it is necessary to restrict the considered time interval in order to adequately represent the variability of the control simulation. As the maximum of the control saturates within a few hundred years (after the start of the hosing simulation at $t = 0$, see Text S5 of the SI) the interval $[0, \tau_c]$ is an adequate period in this respect. The larger the value of γ^I the better the quality of the indicator I; if $\gamma^I \leq 0$ no detection occurs. For example, based on the results in Figure 3a the value of γ^{K_d} for the complete Atlantic MOC field is about 0.07 (see No. 1 in Table 1). Values of γ for both the variance (Figure 3b) and the lag 1 autocorrelation (Figure 3c) are smaller than zero.

The excellent performance of the kurtosis indicator K_d (with a detection time at 738 years, no false alarm, and a positive value of γ^{K_d}) in Figure 3a is shown in entry No.1 in Table 1.

So far, we used the complete Atlantic MOC field of the FAMOUS model data, but at the moment, MOC observations are only routinely made at 26°N through the Rapid Climate Change-Meridional Overturning Circulation and Heatflux Array (RAPID-MOCHA) program [*Cunningham et al.*, 2007]. There are also initiatives to monitor the MOC at 35°S (SAMOC, see www.aoml.noaa.gov/phod/SAMOC_international) and at about 60°N (OSNAP, see www.o-snap.org). Motivated by the fact that current and near-future available observations of the MOC will only be available along zonal sections in the Atlantic, we next reconstructed networks (and the indicator K_d) from limited section MOC data of the FAMOUS model results.

The performance of the kurtosis indicator K_d for different sections and combinations of sections is shown in Table 1. The indicator K_d provides two false alarms and one relatively late alarm for data at 26°N (No. 2 in Table 1), no alarm at all for data at 33°S (No. 3 in Table 1), and does not perform well for all other single section data (see Table S1 in the SI). When the lag 1 autocorrelation and variance of time series averaged over a single section are considered (see Tables S2 and S3 in the SI), the lag 1 autocorrelation performs best at 21°N, although it still gives a false alarm. The variance indicator does not give any warning for all single sections.
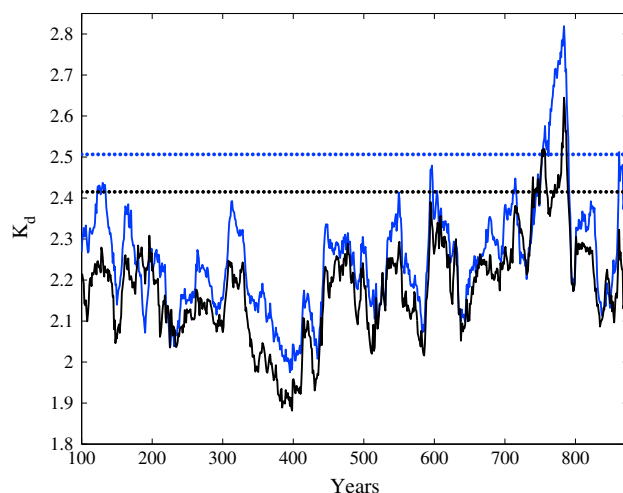
Figure 4. The kurtosis indicator K_d for section data constructed from 21 depth levels and eight latitudes. (a) Data from 31°N, 26°N, 21°N, 16°N, 11°N, 8°S, 13°S, and 18°S (blue solid curve) give the early warning signal at 753 years and last for 38 years. (b) Data from 31°N, 26°N, 21°N, 16°N, 11°N, 13°S, 18°S, and 33°S (black solid curve) give the early warning signal at 740 years and last for 49 years. The dotted blue horizontal line indicates the maximum K_d value of the control simulation of section data (Figure 4a) taken over the total time interval $[0, \tau_c]$, and the dotted black horizontal line indicates the corresponding maximum K_d value of section data (Figure 4) taken over the total time interval $[0, \tau_c]$.

To determine the optimal observation locations of the MOC using K_d, we systematically deleted sections from the complete Atlantic MOC field and evaluated the performance of the indicator K_d for the remaining sections. Entry No. 4 in Table 1 shows that the indicator K_d still works well for the Atlantic MOC field with halved horizontal resolution (21 (depth) × 21 (latitude) = 441 nodes), as well as for the sets of sections including midlatitudes both in the Northern and Southern Hemispheres (Nos. 6–8 in Table 1). However, detection fails for the set of sections located only in the Northern Hemisphere at mid and high latitudes (No. 5 in Table 1).

The most reduced latitude set for which the performance of the indicator K_d is still comparable to the case of the complete Atlantic MOC field (Figure 3a and No. 1 in Table 1) is latitude set I, which consists of 18°S, 13°S, 8°S, 11°N, 16°N, 21°N, 26°N, and 31°N (blue curve in Figure 4 and No. 9 in Table 1). This set consists of 21 (depth) × 8 (latitude) = 168 grid points, and hence, the number of nodes is considerably reduced (by 81%) in comparison to the complete Atlantic MOC field. Further analysis (see Table S4 in the SI) indicates that the data at sections 18°S and 31°N are essential for a good detection of the MOC collapse. In order to examine the importance of monitoring the MOC at 35°S (SAMOC), we substituted 8°S in the latitude set I by 33°S and formed the latitude set II (green curve in Figure 4 and No. 10 in Table 1). The results of Nos. 9 and 10 in Table 1 indicate that including the MOC data at 33°S (near the SAMOC section) would advance the detection time of a future collapse of the MOC compared to including a section at 8°S, but the detection intensity γ^{K_d} of the kurtosis indicator K_d would be slightly decreased.

The physical reason for the optimal observation regions is the following. In ocean-climate models, the MOC collapse is due to a robust feedback involving the transport of salinity by the ocean circulation, the salt advection feedback [*Stommel*, 1961; *Walin*, 1985]. The subtropics are strong evaporation regions, and hence, the largest salinity gradients, central in the salt advection feedback, are located in these regions. Consequently, it is expected that here the strongest response due to the salt advection feedback appears and hence the strongest spatial correlations in the MOC field. Support for this comes from the structure of the dominant EOFs of the equilibrium solutions where the largest amplitude is also located in these midlatitude regions (see Text S4 of the SI).

4. Discussion

Using techniques of complex network theory we have provided a novel indicator which can give an early warning signal for a collapse of the MOC. When applied to data from the FAMOUS model [*Hawkins et al.*, 2011], our results show that when the appropriate midlatitude North and South Atlantic MOC data are available, the kurtosis indicator K_d provides a strong anomalous signal at least 100 years before the transition. Although at the moment a collapse of the MOC is considered a high-impact but low-probability event [*Collins et al.*, 2013], modesty is required regarding our confidence in this statement. The processes controlling the behavior of the MOC, such as the downwelling in the northern North Atlantic boundary currents, are not well represented in many of the climate models on which this statement is based. In state-of-the-art GCMs, such as those used in the IPCC AR5, MOC collapses have not been found yet, but it is fair to say that these models have not been extensively tested for this behavior [*Collins et al.*, 2013; *Huisman et al.*, 2010].

Up to now, there are about 10 years of data on the MOC from the RAPID-MOCHA array, and although this array will likely be operational up to the year 2020, the temporal extent of the time series proceeds only slowly. Due to this insufficient length of the observational record, the indicator K_d is not yet applicable to observational data and hence cannot be used to determine whether the recent downward trend in the observed MOC strength at 26°N [*Smeed et al.*, 2013] is the start of a collapse. Such MOC behavior may just be related to natural variability such as that associated with the Atlantic Multidecadal Oscillation [*Kerr*, 2000; *Knight et al.*, 2005]. However, the strong element of an indicator such as K_d, in contrast to indicators based on a single-point time series, is that it is based on spatial correlations. Our results indicate that an increase in spatial resolution of the MOC observations (i.e., at more sections) can improve early detection using this indicator, because the spatial coherence arising near the transition is better captured. This is another reason that such observations should be given high priority in climate research.

References

Bryan, F. O. (1986), High-latitude salinity effects and interhemispheric thermohaline circulations, *Nature*, *323*, 301–304.

Collins, M., et al. (2013), Long-term climate change: Projections, commitments and irreversibility, in *Climate Change 2013: The Physical Science Basis. Contribution of Working Group I to the Fifth Assessment Report of the Intergovernmental Panel on Climate Change*, edited by T. Stocker et al., pp. 1029–1136, Univ. of Cambridge Press Syndicate, Cambridge, U. K.

Cunningham, S. A., et al. (2007), Temporal variability of the Atlantic Meridional Overturning Circulation at 26.5°N, *Science*, *317*(5840), 935–938.

Dakos, V., S. Kéfi, M. Rietkerk, E. H. van Nes, and M. Scheffer (2011), Slowing down in spatially patterned ecosystems at the brink of collapse, *Am. Nat.*, *177*(6), 154–166.

Donges, J. F., Y. Zou, N. Marwan, and J. Kurths (2009), Complex networks in climate dynamics, *Eur. Phys. J. Spec. Top.*, *174*(1), 157–179.

Feng, Q. Y., and H. Dijkstra (2014), Are North Atlantic multidecadal SST anomalies westward propagating?, *Geophys. Res. Lett.*, *41*, 541–546, doi:10.1002/2013GL058687.

Ganachaud, A., and C. Wunsch (2000), Improved estimates of global ocean circulation, heat transport and mixing from hydrographic data, *Nature*, *408*, 453–457.

Hawkins, E., R. S. Smith, L. C. Allison, J. M. Gregory, T. J. Woollings, H. Pohlmann, and B. De Cuevas (2011), Bistability of the Atlantic overturning circulation in a global climate model and links to ocean freshwater transport, *Geophys. Res. Lett.*, *38*, L10605, doi:10.1029/2011GL047208.

Huisman, S. E., M. den Toom, H. A. Dijkstra, and S. Drijfhout (2010), An indicator of the multiple equilibria regime of the Atlantic Meridional Overturning Circulation, *J. Phys. Oceanogr.*, *40*(3), 551–567.

Johns, W., M. Baringer, and L. Beal (2011), Continuous, array-based estimates of Atlantic Ocean heat transport at 26.5°N, *J. Clim.*, *24*, 2429–2449.

Kerr, R. A. (2000), A North Atlantic climate pacemaker for the centuries, *Science*, *288*, 1984–1986.

Knight, J. R., R. J. Allan, C. K. Folland, M. Vellinga, and M. E. Mann (2005), A signature of persistent natural thermohaline circulation cycles in observed climate, *Geophys. Res. Lett.*, *32*, L20708, doi:10.1029/2005GL024233.

Lenton, T. M. (2011), Early warning of climate tipping points, *Nature Climate Change*, *1*(4), 201–209.

Lenton, T. M., H. Held, E. Kriegler, J. W. Hall, W. Lucht, S. Rahmstorf, and H. J. Schellnhuber (2008), Tipping elements in the Earth's climate system, *Proc. Nat. Acad. Sci.*, *105*(6), 1786–1793.

Livina, V. N., and T. M. Lenton (2007), A modified method for detecting incipient bifurcations in a dynamical system, *Geophys. Res. Lett.*, *34*, L03712, doi:10.1029/2006GL028672.

Mheen, M., H. A. Dijkstra, A. Gozolchiani, M. den Toom, Q. Feng, J. Kurths, and E. Hernandez-Garcia (2013), Interaction network based early warning indicators for the Atlantic MOC collapse, *Geophys. Res. Lett.*, *40*, 2714–2719, doi:10.1002/grl.50515.

Rahmstorf, S. (2000), The thermohaline circulation: A system with dangerous thresholds?, *Clim. Change*, *46*, 247–256.

Scheffer, M., J. Bascompte, W. A. Brock, and V. Brovkin (2009), Early-warning signals for critical transitions, *Nature*, *461*(7260), 53–59.

Smeed, D. A., et al. (2013), Observed decline of the Atlantic meridional overturning circulation 2004 to 2012, *Ocean Sci. Discuss.*, *10*(5), 1619–1645.

Stommel, H. (1961), Thermohaline convection with two stable regimes of flow, *Tellus*, *2*, 244–230.

Tietsche, S., D. Notz, J. H. Jungclaus, and J. Marotzke (2011), Recovery mechanisms of Arctic summer sea ice, *Geophys. Res. Lett.*, *38*, L02707, doi:10.1029/2010GL045698.

Tsonis, A. A., and P. J. Roebber (2004), The architecture of the climate network, *Physica A*, *333*, 497–504.

Tsonis, A. A., and K. L. Swanson (2006), What do networks have to do with climate?, *Bull. Am. Meteorol. Soc.*, *87*(5), 585–595.

Viebahn, J., and H. A. Dijkstra (2014), Critical transition analysis of the deterministic wind-driven ocean circulation—A flux-based network approach, *Int. J. Bifurcation Chaos*, *24*(02), 1430007.

Walin, G. (1985), The thermohaline circulation and the control of ice ages, *Paleogeogr. Paleoclim. Paleoecol.*, *50*, 323–332.